

## Advances in the physics basis for the European DEMO design

This content has been downloaded from IOPscience. Please scroll down to see the full text.

2015 Nucl. Fusion 55 063003

(<http://iopscience.iop.org/0029-5515/55/6/063003>)

View [the table of contents for this issue](#), or go to the [journal homepage](#) for more

Download details:

IP Address: 181.46.17.126

This content was downloaded on 25/06/2016 at 23:58

Please note that [terms and conditions apply](#).

# Advances in the physics basis for the European DEMO design

R. Wenninger<sup>1,2</sup>, F. Arbeiter<sup>3</sup>, J. Aubert<sup>4</sup>, L. Aho-Mantila<sup>5</sup>,  
R. Albanese<sup>6</sup>, R. Ambrosino<sup>7</sup>, C. Angioni<sup>2</sup>, J.-F. Artaud<sup>8</sup>,  
M. Bernert<sup>2</sup>, E. Fable<sup>2</sup>, A. Fasoli<sup>9</sup>, G. Federici<sup>1</sup>, J. Garcia<sup>8</sup>,  
G. Giruzzi<sup>8</sup>, F. Jenko<sup>2</sup>, P. Maget<sup>8</sup>, M. Mattei<sup>10</sup>, F. Maviglia<sup>1,6</sup>,  
E. Poli<sup>2</sup>, G. Ramogida<sup>11</sup>, C. Reux<sup>8</sup>, M. Schneider<sup>8</sup>, B. Sieglin<sup>2</sup>,  
F. Villone<sup>12</sup>, M. Wischmeier<sup>2</sup> and H. Zohm<sup>2</sup>

<sup>1</sup> EUROfusion Programme Management Unit, Boltzmannstraße 2, D-85748 Garching, Germany

<sup>2</sup>Max-Planck-Institut für Plasmaphysik, Garching, Germany

<sup>3</sup>Karlsruhe Institute of Technology, Karlsruhe, Germany

<sup>4</sup>CEA-Saclay, DEN/DM2S/SEMT, 91191 Gif-Sur-Yvette, France

<sup>5</sup>VTT Technical Research Centre of Finland, PO Box 1000, FI-02044 VTT, Finland

<sup>6</sup>Università di Napoli Federico II, Corso Umberto I, 40bis, 80138 Napoli, Italy

<sup>7</sup>Università di Napoli Parthenope, Via Medina, 40, 80133 Napoli, Italy

<sup>8</sup>CEA, IRFM, F-13108 St Paul-Lez-Durance, France

<sup>9</sup>CRPP, EPFL, CH - 1015 Lausanne, Switzerland

<sup>10</sup>DIIN, Seconda Università di Napoli, Via Antonio Vivaldi, 43, 81100 Caserta CE, Italy

<sup>11</sup>C.P. 65-I-00044-Frascati, Rome, Italy

<sup>12</sup>Università di Cassino, Viale dell'Università, 03043 Cassino, Italy

E-mail: [ronald.wenninger@euro-fusion.org](mailto:ronald.wenninger@euro-fusion.org)

Received 19 December 2014, revised 16 February 2015

Accepted for publication 20 March 2015

Published 30 April 2015



CrossMark

## Abstract

In the European fusion roadmap, ITER is followed by a demonstration fusion power reactor (DEMO), for which a conceptual design is under development. This paper reports the first results of a coherent effort to develop the relevant physics knowledge for that (DEMO Physics Basis), carried out by European experts. The program currently includes investigations in the areas of scenario modeling, transport, MHD, heating & current drive, fast particles, plasma wall interaction and disruptions.

Keywords: DEMO, scenario, transport, MHD, fast particles, PWI, disruption

(Some figures may appear in colour only in the online journal)

## 1. Introduction

In the European fusion roadmap [1] ITER is followed by a demonstration fusion power plant (DEMO) [2], with the capability of generating several hundred MW of net electricity and operating with a closed fuel-cycle. The development of a conceptual design of DEMO is one of the main priorities of the European fusion program in this decade. This activity implies extensive engineering efforts dedicated to the overall machine design and the design of individual machine components (e.g. breeding blanket or divertor). Related to these tasks is also a variety of open questions in the area of physics and at the

interface between physics and engineering that need to be addressed.

In comparison to the ITER ( $Q = 10$ ) design the European DEMO design options have significantly higher fusion power, higher normalized plasma beta  $\beta_N = \beta a B / I_p$ , higher temperature across the whole profile, higher fuelling rate and higher core radiation fraction. Hence, beside some simplifications of requirements (e.g. as DEMO will be a point design), more challenging conditions in various fields will have to be faced. Therefore it is important to obtain a good perception of a number of aspects of the physics of DEMO, which are related to the feasibility and the performance of the device. The relevant physics knowledge, referred to as *DEMO Physics Basis*, is important for two main reasons. Firstly, it is crucial to develop design points [3] which are consistent not only on the overall level but also in a reasonable level of detail.



Content from this work may be used under the terms of the [Creative Commons Attribution 3.0 licence](https://creativecommons.org/licenses/by/3.0/). Any further distribution of this work must maintain attribution to the author(s) and the title of the work, journal citation and DOI.

Secondly, there are a number of projects that are developing concept designs for DEMO components, which require the knowledge of boundary conditions (e.g. thermal loads), under which these components have to operate. The program to develop the DEMO Physics Basis, which was launched in 2014, is carried out by European experts from several labs. It is based on an earlier assessment [4] and will be expanded as further relevant areas are identified. Currently the following areas are investigated: scenario modeling, transport, MHD, heating & current drive, fast particles, plasma wall interactions, disruptions.

This paper will briefly introduce most of these areas and report initial results. For the area *scenario modeling* we refer to [5]. Due to the early phase of this development, the paper is not meant to provide a systematic overview of the DEMO Physics Basis, but rather an impression of the research questions in this area based on a number of examples.

## 2. Transport

This area concentrates on fundamental questions of plasma transport, which are important when simulating DEMO scenarios. A central topic is the prediction of the energy confinement time  $\tau_E$  in DEMO. The standard approach for such a prediction is using a confinement time scaling. However, it has been noted that the envisaged DEMO operational point lies outside the region of confidence in input parameters for the IPB98(y,2) scaling for at least  $\beta$ , Greenwald density fraction  $\langle n_e \rangle / n_{GW}$  and total radiation fraction  $P_{rad} / P_{heat,tot}$  [4]. We support the proposed development of a more DEMO relevant scaling based on a more appropriate dataset and alternative, theory-based fit functions [4].

Due to the uncertainty associated with scalings, a complementary approach of predicting  $\tau_E$  is proposed. It starts with a prediction of the pedestal height employing typical methods (section 3.2). This height is used as boundary condition for a core transport calculation employing the core transport module TGLF [6], from which  $\tau_E$  can be deduced. As an example, figure 1 shows the dependence of the confinement factor on the electron temperature at the pedestal top. In contrast to the application of a confinement time scaling, the attractive feature of this approach is that the uncertainties are more isolated in local areas (e.g. plasma pedestal, plasma core).

Following other investigations started or on-going in this area are:

- In DEMO relatively strong impurity seeding will need to be applied (section 6.1). For this reason the transport of impurities is of central interest. Simulations employing an approach [7] that is using a coupling of a neoclassical and a turbulent code, are planned.
- The question of the optimum density profile in DEMO, which can be achieved (pellet fuelling) and stably maintained at acceptable confinement, has a direct link to the performance of the device. Based on recent progress in the field of density limits [8, 9] investigations with the ultimate goal to arrive at predictions of the DEMO density limits with reasonable reliability are being carried out.
- The core transport model TGLF [6] has been validated on various machines [10, 11]. Due to this and due to the possibility to run TGLF at the expense of relatively

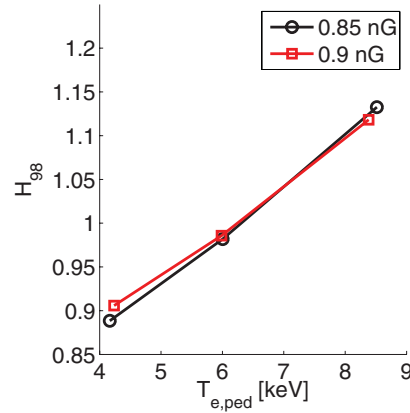


**Figure 1.** Dependence of radiation corrected confinement factor (the power injected to the H98 scaling is  $P_{heat,tot} - P_{rad,core}$ ) on the electron temperature at the pedestal top from calculations with the core transport module TGLF [6]. The electron density at the pedestal top has been set to 85 and 90% of the Greenwald density respectively.

modest resources, it is an attractive tool for DEMO studies. Considering the high electron pressure ( $\beta_e \approx 1\%$ ) and fast particle fraction ( $p_\alpha / p_{th} \leq 0.7$ ) in DEMO, it remains to be examined, if it is appropriate to use TGLF to simulate this device. To resolve this, gyro-kinetic simulations of DEMO plasmas are performed to compare their results to TGLF.

## 3. MHD

MHD related activities mainly investigate limits that have to be respected in order to avoid various types of instabilities. In this section initial results in three key areas are presented. Beyond this it is crucial to identify candidates of scenarios with no or only tolerable edge localized modes (ELMs) in DEMO [12]. We remind that also a robust design integration concept needs to be developed for any tool to mitigate ELMs in such a scenario.

### 3.1. Beta limit

The question of the achievable total  $\beta$  is of key importance for the prediction of the performance of DEMO design option. It is currently assumed that a technique to control neoclassical tearing modes (NTMs) is implemented in the control concept, in favor of optimizing  $\beta$ . New results on the power required for this are reported in section 4. The  $\beta$  limit for the pulsed European DEMO design has been investigated by linear stability analysis [13] after suppressing the  $q = 1$  surface. The far-wall limit ( $b/a = 3$ ,  $a$ : minor radius,  $b$ : position of an ideal wall) is around  $\beta_N = 3.1$ . With an ideally conducting wall at  $b/a = 1.5$  that corresponds to the position of the inner vessel shell, the  $n = 1$  mode is stable up to  $\beta_N = 4.1$ . In comparison, the values of the recent European designs, which are determined by the confinement, are:  $\beta_N = 2.5$ –3 (pulsed) and  $\beta_N = 3.4$ –3.8 (steady-state).

### 3.2. Edge stability

The stability of the pedestal is investigated by similar methods [13] and by independently modifying the pressure gradient

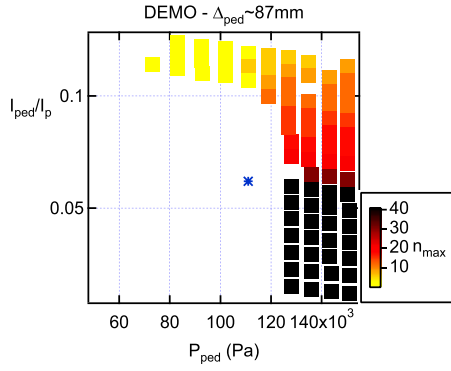


**Figure 2.** Most unstable mode number as a function of pedestal pressure and pedestal current fraction: The  $\star$  marks the unmodified situation.

and current in the pedestal region, starting from an equilibrium where the current density in the pedestal has been replaced by a self-consistent computation of the bootstrap current, using the Sauter formula [14]. The pedestal width has been prescribed to be  $\Delta\psi = 7\%$  in normalized units, which corresponds to approximately 87 mm. This corresponds to about 3.5% of the minor radius in real space, a ratio that is similar to the one used for recent ITER simulations [13] and the ones observed in many experiments [15].

Ideal instabilities with toroidal mode numbers between 3 and 40 have been investigated. Figure 2 displays the resulting stability diagram, in which the ballooning limit is found around 130 kPa for the prescribed pedestal width, which is equivalent to  $15 \text{ kPa cm}^{-1}$ . Assuming a pedestal top density of 85% of the Greenwald density limit, this corresponds to a pedestal top temperature of 5.6 keV.

### 3.3. Vertical stability

The stability against vertical displacement events poses a boundary condition on the maximum elongation and hence on the total plasma performance. In the standard European DEMO design this is particularly restrictive, as the plasma is separated from toroidally conducting structures by a 1 m thick blanket. The dependence of the maximum elongation on the aspect ratio has been studied with a fully consistent approach, in which for three aspect ratios a system code solution and a 2D design of the main components have been developed. Based on this, passive and active stability properties have been analyzed using the codes CREATE-NL [16] and CREATE-L [17]. For each aspect ratio this analysis has been carried out for the flat top phase (FT) and the start of the ramp-down after the H-L-transition (SRD). A toroidally symmetric design with conducting vessel shells and no other conducting structures has been considered. The neglected effect of the breeding blanket is estimated to be small and stabilizing.

The passive stability parameters for FT are illustrated in figure 3. The stability margin  $m_s$ , which is recommended to be at least 0.3 [18], has been evaluated assuming conservation of poloidal flux during the vertical displacement event. It increases with decreasing elongation and decreasing aspect ratio  $A$ . Table 1 shows the elongations at the surface of 95% of poloidal flux  $k_{95}$  corresponding to  $m_s = 0.3$ . Due to higher values of  $\beta$  and lower values of  $li$  the maximum achievable

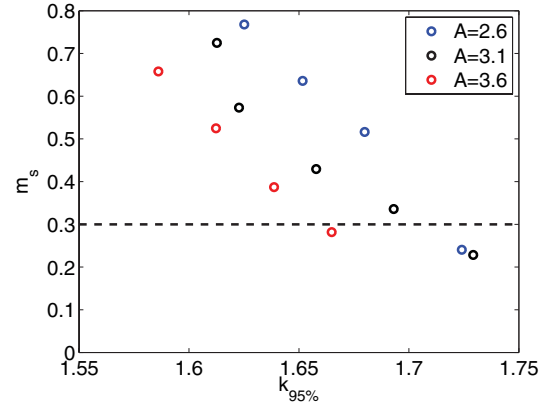


**Figure 3.** Stability margin  $m_s$  evaluated at constant poloidal flux versus elongation at  $\rho_{pol} = 0.95$  for three aspect ratios  $A$  at FT.

**Table 1.** Vertical stability as a function of the aspect ratio and discharge phase:  $k_{95}$  corresponding to  $m_s = 0.3$  evaluated at constant poloidal flux and  $P_{re}$  for this elongation and two types of perturbations.

	A	2.6	3.1	3.6
	$I_p$ [MA]	24.2	20.3	17.7
FT	$k_{95}$ at $m_s = 0.3$	1.72	1.71	1.66
	$P_{re}$ for 5 cm VDE [MW]	100	240	240
	$P_{re}$ for 100 MJ ELM [MW]	>600	>600	>600
SRD	$k_{95}$ at $m_s = 0.3$	1.65	1.59	1.56
	$P_{re}$ for 5 cm VDE [MW]	80	200	250
	$P_{re}$ for $\Delta li = 0.09$ [MW]	400	>600	>600

elongations respecting the criterion  $m_s \geq 0.3$  are higher for FT than for SRD.

For the analysis of the active stabilization features an uncontrolled 5 cm vertical displacement event (VDE) has been considered. Additionally, for FT the perturbation corresponding to a 100 MJ ELM [12] and for SRD a perturbation corresponding to  $\Delta li = 0.09$ , as observed in extreme cases in the JET ramp-down, have been considered. The required installed power  $P_{re}$  is estimated based on a voltage equivalent to twice the required control voltages to stabilize these perturbations at  $t = \infty$  (table 1). Scaling up the installed power for vertical stabilization from ITER to DEMO gives about 300 MW. Table 1 shows that  $P_{re}$  is beyond reasonable values for  $A \geq 3.1$  assuming the stronger perturbations and the standard European DEMO design. This motivates the investigation of toroidally asymmetric design concepts leading to toroidally conducting structures closer to the plasma. A deeper analysis should also investigate changes of  $li$  during SRD and their dynamics. Additionally, table 1 shows that type I ELMs in DEMO not only pose a severe problem in terms of power exhaust [12] but also in terms of vertical stabilization for all aspect ratios.

## 4. Heating & current drive

Heating & Current Drive (HCD) systems in DEMO will have a number of functions. Initial studies of the physics of HCD in DEMO have concentrated on the capability of several candidate systems to drive current in the flat top

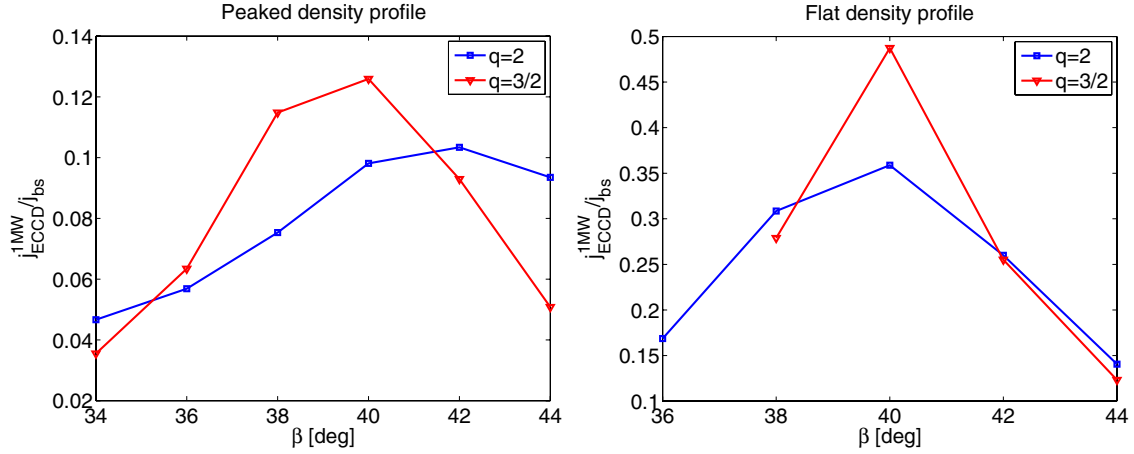


**Figure 4.** Ratio between ECCD current density and bootstrap current density at the position of the  $q = 3/2$  and  $q = 2$  surfaces, assuming 1MW injection, for flat and peaked density profiles as a function of toroidal injection angle  $\beta$ .

phase of the discharge [19]. In order to optimize the achievable  $\beta$  and hence the overall performance of the device, ECRH systems can be used to control NTMs. While ECE systems, which are likely to be applicable in DEMO [20], are foreseen as central diagnostics for the detection and location of the mode, a detailed control scheme has not yet been elaborated.

A first study of the power required for NTM stabilization has been performed for a pulsed DEMO design with a major radius  $R_0 = 9$  m and an aspect ratio  $A = 4$ . Due to the uncertainty in the prediction of kinetic profile in DEMO two different sets of kinetic profiles have been employed, one corresponding to flat density inside the H-mode pedestal (peaking factor  $n_{e0}/\langle n_e \rangle = 1.1$ ), the other one to more significant peaking ( $n_{e0}/\langle n_e \rangle = 1.5$ ). While the fusion power varies by about 10% in the two cases, the value of  $\beta_N$  has been kept approximately constant ( $\beta_N \approx 2.2$ ). Therefore the flat-density case corresponds to higher core temperature ( $T_{e0} = 26$  keV) as compared to the peaked-density case ( $T_{e0} = 19$  keV) [19]. Since the current drive efficiency scales roughly as  $T_e/n_e$ , a better performance in terms of power required for NTM stabilization can be expected for the flat density case. The equilibrium features quite a central radial location for the rational surfaces most prone to NTMs, namely  $\rho_{\text{pol}} = 0.4$  (resp. 0.6) for the  $q = 3/2$  (resp.  $q = 2$ ) surfaces in the flat-density case and  $\rho_{\text{pol}} = 0.46$  (resp. 0.66) in the peaked-density case,  $\rho_{\text{pol}}$  representing the normalized poloidal radius. The frequencies and the launch locations chosen for the present assessments are those with the highest peak current drive efficiency, as found through an analysis similar to that presented in [21]. This optimization leads to an elevated launcher position and high wave frequencies, namely  $(R, Z) = (10.5, 3)$  m and 280 GHz for the flat-density and  $(R, Z) = (11, 2.5)$  m and 270 GHz for the peaked-density case [19].

Our calculations have been performed employing the beam tracing code TORBEAM [22]. The beams are launched assuming that they leave the antenna with a flat phase front, since no focusing mirror is likely to be placed at the plasma end of the transmission system (an optimization of the focusing would reduce the profile width by a factor around

1.5). At these frequencies, an initial beam width of 4.6 cm, as employed here, does not lead to significant diffractive broadening. Nevertheless, the typical ECCD profiles found in our calculations range between about 8 and 12 cm, depending on the profiles and on the rational surface under consideration.

According to [23], when the ECCD profile width is larger than the expected width of the (marginal) magnetic island just before suppression, NTM stabilization can be achieved with modulated injection at the island O-point if the EC driven current density  $j_{\text{cd}}$  exceeds by about 20% the unperturbed bootstrap current density  $j_{\text{bs}}$  at the surface of interest. We have hence performed an angular scan to identify the combination of toroidal and poloidal angles which maximizes the current density driven by the EC waves. Figure 4 shows the ratio between  $j_{\text{cd}}$  and  $j_{\text{bs}}$  at the position of the  $q = 3/2$  and  $q = 2$  surfaces, assuming 1 MW injection, for flat and peaked profiles as a function of the toroidal injection angle  $\beta$  (the corresponding poloidal injection angle is determined so that the peak current density is driven at the rational surface of interest). The injection power required to reach  $j_{\text{cd}}/j_{\text{bs}} > 1.2$  is found to be 2.5 MW (resp. 3.3 MW) for the  $q = 3/2$  (resp.  $q = 2$ ) surface in the flat-density case and 9.5 MW (resp. 11.6 MW) for the peaked-density case. These relatively modest requirements as compared e.g. with a system optimized for NTM control as the ITER upper launcher [24, 25] are basically due to the higher gyrotron frequency adopted in this analysis. It should be stressed, however, that even a somewhat lower frequency (say 240 GHz) would not change significantly the present results, as this would move the resonance on slightly less energetic electrons, but increase the absorption coefficient, thus reducing the ECCD profile width. A more thorough analysis is planned for the near future, and is likely to reduce the values reported above even further. However, it is unrealistic that the ECCD profile width can be reduced below the marginal island width, since even in the presence of focusing other effects, like beam scattering from density fluctuations would likely spoil the achieved focusing (see e.g. [26]). As explained above, this implies that power modulation should be foreseen in an ECCD-based NTM stabilization scheme in DEMO.



## 5. Fast particles

All fast ion issues that are presently under scrutiny for ITER are of relevance for DEMO. However, in DEMO alpha particles will be providing by far the dominating component of the plasma heating mix (ITER:  $P_\alpha/P_{\text{heat,tot}} \approx 0.66$ , European pulsed DEMO:  $P_\alpha/P_{\text{heat,tot}} \approx 0.91$ ). Understanding and controlling fast ions in DEMO will therefore be even more important than in ITER.

The fast ion beta contribution  $\beta_{\text{fast}}/\beta_{\text{tot}}$  will be 0.2–0.4 assuming the European DEMO designs, which compares to 0.2–0.3 in ITER. Hence  $\beta_{\text{fast}}$  is becoming an important fraction of the total beta and the question of the effect of  $\beta_{\text{fast}}$  on the total  $\beta$  limit arises. Arguably, one of the most crucial issue for fast ions in DEMO remains the resonant interaction with MHD modes, with the possible destabilization of the modes and their effect on the fast ion redistribution and losses. Central redistribution influences all plasma profiles and affects the fusion performance, via an effect on the He ash accumulation and the D-T mix.

The highest priority for the safety of the machine is to avoid fast ion losses. Loss fractions as small as a few percent can in fact lead to significant localized damages. The questions to address are therefore in which condition the linear stability, resulting from the balance between damping and drive, is achieved for the modes that could lead to these losses, and, if linear stability cannot be guaranteed, what would be the nonlinear evolution of these modes and the resulting effect on the fast ion orbits. Also limits of acceptable magnetic inhomogeneity need to be established.

The main challenge in the prediction of fast particle effects for DEMO is that present experiments cannot be used to validate the models in the specific DEMO conditions, i.e. with large values of  $\beta_{\text{fast}} \sim \beta_{\text{plasma}}$ , and very small values of the ratio between the fast ion orbit size and the plasma radius  $\rho_{L,\text{fast}}^*$ . The former condition implies that strong, potentially dangerous, modes are driven inside the Alfvén continuum. The fact that  $\rho_{L,\text{fast}}^* \ll 1$  is expected to lead to regimes characterized by a sea of many short wavelength, nonlinearly interacting modes, and the possibility of overlaps in the wave-particle resonances in phase space, leading to transport over extended regions even when each individual mode is restricted to a very limited portion of the plasma profile.

## 6. Plasma wall interaction

Finding a solution for handling the power and particle exhaust in DEMO is one of the ultimate challenges within the European fusion roadmap. For both divertor and first wall the agreement of achievable load limits and predicted loads need to be addressed.

The current baseline strategy for the DEMO divertor assumes a conventional divertor operating at a similar value of the divertor challenge quantifier  $P_{\text{sep}}/R$  [12, 27] as ITER ( $P_{\text{sep}}$ : loss power across the separatrix) and a significantly higher core radiation fraction. However, it is not completely obvious that a conventional x-point divertor configuration with ITER-like divertor technology can withstand the steady state and dynamical loads in DEMO. A first, but not complete, assessment of the divertor limitations in DEMO has been

made [12]. One of the central problems in this context is a lack of capability to reliably predict the behavior of the divertor of future devices. Also it should be noted that there is a substantial European program in support of alternative divertor solutions.

### 6.1. Divertor protection

In favour of divertor protection, it is obvious that a significant part of the power that is leaving the plasma needs to be radiated, as this leads to a more homogeneous distribution of the power to the plasma facing components. To achieve this relatively strong impurity, seeding needs to be applied. There is a concern that particularly the high amount of core radiation might be in conflict with the operation in H-mode. Based on the double radiation feedback experiment in ASDEX Upgrade [27] we have investigated the optimum impurity mix to fulfil the following criteria:

- The power reaching both divertor targets in total needs to be below a threshold  $P_{\text{div,tol}}$  (Default: 30 MW [12]).
- The loss power across the separatrix must be above the LH threshold power  $P_{\text{LH}}$  [28].
- The fusion power is maximized.

The investigation is done with a similar setup as the evaluation of the W sputtering limit in [12]. Background profiles are generated for a pulsed DEMO design option with the transport code ASTRA [29, 30] using TGLF [6] as core transport model. The effect of dilution on these background profiles is not accounted for. For combinations of the impurity species N, Ne, Ar, Kr and Xe the impurity concentrations are scanned assuming constant impurity concentrations across the confined plasma and in the SOL with a default ratio  $c_{\text{imp,SOL}}/c_{\text{imp,core}}$  of 3. For the Helium concentration  $c_{\text{He}} = 5 \times 10^{-2}$  and for the W concentration  $c_{\text{W}} = 10^{-5}$  have been used as default values.

Based on this the fusion power, the power to Bremsstrahlung and the synchrotron radiation power are calculated. The line radiation power for all impurities in the plasma is evaluated using radiative loss functions calculated on the basis of data from ADAS [31]. The power radiated in the SOL and divertor  $P_{\text{rad,SOL}}$  is calculated employing the same method as described in [12] using the same radiative loss functions as mentioned above. For the non-coronality parameter  $n_e \tau$  [32] a default value of  $1000 \times 10^{20} \text{ m}^{-3} \times \text{ms}$  has been used, which is close to the assumption of coronal equilibrium. This method neglects a number of relevant physics mechanisms such as momentum loss processes in the SOL and hence it is assumed that it underestimates  $P_{\text{rad,SOL}}$ .

With the default parameters, criteria (a) and (b) can be satisfied simultaneously only for pure Ar or the mixtures Ar/Kr and Ar/Xe. The highest fusion power is obtained with Ar/Xe (figure 5). Due to dilution, increasing the concentration of either impurity species leads to a reduction of the fusion power. The lines representing the limits of satisfying criteria (a) and (b) are crossing under a very small angle, which is corresponding to a very limited operation window. The optimum impurity mix marked by the blue circle in figure 5 (0.74% Ar and 0.013% Xe) allows for 64% core radiation fraction.

The assumptions made in this analysis are associated with significant uncertainties. The essential ones are related to  $P_{\text{LH}}$ ,  $P_{\text{rad,SOL}}$ ,  $P_{\text{div,tol}}$ ,  $c_{\text{W}}$ ,  $c_{\text{He}}$  and  $c_{\text{imp,SOL}}/c_{\text{imp,core}}$ . Some of these

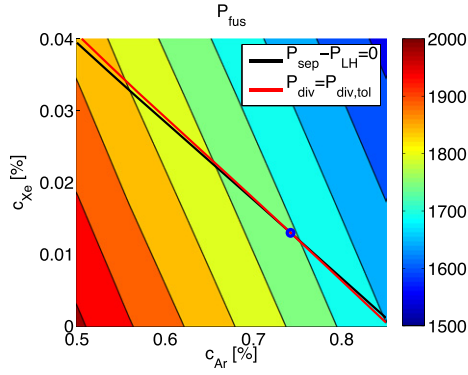


**Figure 5.** Investigation of the optimum impurity mix of Ar and Xe. Contour levels illustrate fusion power. The red and black lines show the limits of satisfying criterion (a) and (b). The blue circle marks the identified optimum impurity mix.

parameters, and in particular  $c_W$  and  $c_{He}$ , have the potential to substantially impact the fusion power up to a point where the burn condition is not fulfilled anymore. Also it is not clear yet, if species like Ar, Kr or Xe are acceptable in terms of safety in a fusion reactor. Furthermore there is no consideration of pedestal transport effects like the ones leading to different confinement levels for different seeding species, as observed in JET and ASDEX Upgrade. Consequently, the result of this analysis is not the determination of the impurity mix for DEMO, but rather the finding that the existence of a design point satisfying simultaneously the criteria mentioned above is marginal. A solution would be to increase the major radius at constant fusion power.

## 6.2. Wall protection

The loads to the main chamber wall of DEMO represent another area, in which significant progress is necessary. In DEMO, and even more pronounced in following fusion power reactors, the requirements of electric power generation and of tritium self-sufficiency, together with the thermal and mechanical performance limits of available (structural) materials, effect a limitation to the allowable heat flux density of the first wall. These limits are estimated to be at most  $1.5 \text{ MW m}^{-2}$  for water cooling and at most  $1.0 \text{ MW m}^{-2}$  for He cooling. A key parameter to this issue is the coolant exit temperature, which is chosen considerably higher in DEMO (compared to ITER) to allow efficient power generation and to exceed the elevated ductile to brittle transition temperature for the intended end-of-life structural damage.

Hence, it is important to understand the conditions to which the first wall of DEMO will be exposed. It is intended to develop a DEMO Wall Load Specification, which should include poloidally resolved estimates of following load types:

- Stationary loads due to: (1) thermal charged particles (majority/impurities), (2) blobs, (3) radiation / MARFES, (4) neutrals (5) fast particles
- Dynamic loads due to: (1) limiter configuration during ramp-up/down, (2) ELM filaments, (3) confinement transients (e.g. H-L-transition), (4) vertical displacement events / disruptions

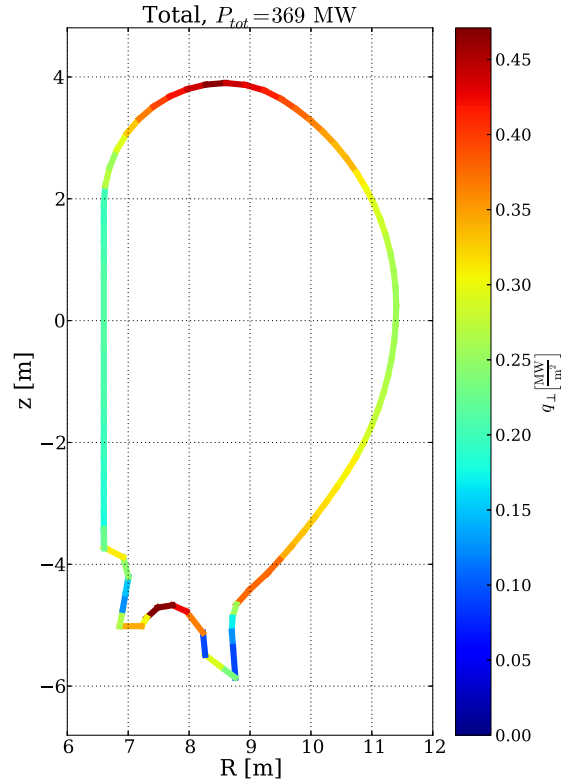


**Figure 6.** Poloidal distribution of the total radiation in DEMO based on a pulsed DEMO design with 0.74% Ar and 0.013% Xe.

For example, initial results on the poloidal distribution of the radiated power onto the first wall of DEMO are presented. This analysis is based on the optimum seeding scenario described above (0.74% Ar and 0.013% Xe), which implies constant impurity densities on flux surfaces. Figure 6 shows the poloidal distribution of the total radiation consisting of radiation due to D/T, Ar, Xe and W from inside and outside the separatrix taking into account the toroidal geometry. In this situation a maximum total radiation power density  $q$  of about  $0.45 \text{ MW m}^{-2}$  is predicted. The poloidal peaking has a value of  $q_{\max}/q_{\text{av}} \approx 2$ . This calculation has been performed under the assumption that the wall absorbs all incident radiation. For a realistic wall, reflections have to be taken into account, therefore a reduction of the peaking factor is likely.

## 7. Disruptions

Disruptions are associated with extensive electromagnetic, mechanical and thermal loads. Hence they pose a significant hazard to the availability and the lifetime of DEMO. In [20] a very rough calculation of the heat impact factor during the thermal quench of a disruption  $\eta_{\text{TC}} = \Delta W_{\text{TC}}/A\sqrt{\tau_{\text{TC}}}$  has been performed, where  $\Delta W_{\text{TC}} \approx 0.5W_{\text{kin}}$  is the kinetic energy loss during the thermal quench phase,  $A$  is the surface area it is released to and  $\tau_{\text{TC}}$  is the thermal quench duration ( $\Delta W_{\text{TC}} \approx 1 \text{ GJ}$  and  $A \approx 1200 \text{ m}^2$  for the pulsed European DEMO design). For  $\tau_{\text{TC}}$  values of 1–3 ms have been assumed, which is roughly in line with extrapolations of  $\tau_{\text{TC}}$  to DEMO presented in [33]. It has to be noted that there is a significant uncertainty on any extrapolation of  $\tau_{\text{TC}}$ , as the thermal quench

is governed by an MHD event, which currently is poorly understood.

Assuming a perfectly mitigated disruption (i.e. no toroidal or poloidal peaking) a value of  $\eta_{TC}$  has been calculated, which is only marginally below the lower threshold for crack formation in W. Hence, even a perfectly mitigated disruption might be unacceptable in DEMO. This leads to the question, should the DEMO design point be moved further towards the low-disruptivity-region in the space spanned by density and safety factor when compared to ITER.

Compared to ITER, DEMO has some significant differences in the design. The lower power flux density limit on the first wall (section 6.2) and the radial extension of the blanket are important in the context of disruptions. In order to understand the effect of these differences a special program [33] consisting of the following main elements has been started:

- Estimation of the main parameters characterizing the plasma evolution during relevant types of disruptions in DEMO
- Simulation of the plasma evolution during disruptions in DEMO with a code, that is self-consistently coupling the nonlinear plasma axisymmetric evolution with volumetric conducting structures (3D)
- Evaluation of the resulting electromagnetic forces on several types of machine components
- Calculation of the resulting evolution of the heat load to plasma facing components

## 8. Conclusions and prospects

It is intended to systematically develop the DEMO Physics Basis in areas, which are crucial for the performance and the feasibility of the device. In this paper we have introduced most of the areas of the DEMO Physics Basis that are currently under development. Also first results have been presented. It is obvious that significantly more work is required. This includes experiments in DEMO-relevant regimes, modeling of various aspects of DEMO physics with state-of-the-art tools and development of theoretical models in areas, where appropriate tools do not yet exist.

These activities towards the DEMO Physics Basis should also help to address key questions beyond ITER at the physics-technology-interface, which need to be resolved on the way to a conceptual design of DEMO. One set of these key questions concern the economically optimal way to design and operate DEMO such that (1) the load on the divertor due to edge instabilities; (2) the steady state load on the divertor; (3) the steady state and dynamical loads on the first main chamber wall and; (4) the risk and impact of disruptions are all acceptable.

Further input of relevant specialists with respect to the scope of investigations and the methods to employ will be very much appreciated.

## Acknowledgments

This work has been carried out within the framework of the EUROfusion Consortium and has received funding from the European Union's Horizon 2020 research and innovation programme under grant agreement number 633053. The views and opinions expressed herein do not necessarily reflect those of the European Commission.

## References

- [1] Romanelli F. *et al* 2012 Fusion electricity: a roadmap to the realisation of fusion energy *Fusion Electricity (EFDA)* (November 2012) [www.fire.pppl.gov/EU\\_Fusion\\_Roadmap\\_2013.pdf](http://www.fire.pppl.gov/EU_Fusion_Roadmap_2013.pdf)
- [2] Federici G. *et al* 2014 *Fusion Eng. Des.* **89** 882–9
- [3] Kemp R. *et al* 2015 *Nucl. Fusion* submitted
- [4] Zohm H. *et al* 2013 *Nucl. Fusion* **53** 073019
- [5] Giruzzi G. *et al* 2015 *Nucl. Fusion* submitted
- [6] Staebler G.M., Kinsey J.E. and Waltz R.E. 2007 *Phys. Plasmas* **14** 055909
- [7] Angioni C. *et al* 2014 *Nucl. Fusion* **54** 083028
- [8] Bernert M. *et al* 2013 *40th EPS Conf. on Controlled Fusion and Plasma Physics* (Espoo, Finland, 1–5 July 2013) <http://ocs.ciemat.es/EPS2013PAP/pdf/P5.163.pdf>
- [9] Bernert M. *et al* 2015 *Plasma Phys. Control. Fusion* **57** 014038
- [10] Kinsey J.E., Staebler G.M. and Waltz R.E. 2008 *Phys. Plasmas* **15** 055908
- [11] Sommer F. *et al* 2012 *Nucl. Fusion* **52** 114018
- [12] Wenninger R. *et al* 2014 *Nucl. Fusion* **54** 114003
- [13] Maget P. *et al* 2013 *Nucl. Fusion* **53** 093011
- [14] Sauter O., Angioni C. and Lin-Liu Y.R. 1999 *Phys. Plasmas* **6** 2834–9
- [15] Beurskens M.N.A. *et al* 2011 *Phys. Plasmas* **18** 056120
- [16] Albanese R. *et al* 2003 *11th Int. Symp. on Applied Electromagnetics and Mechanics* (Versailles, France, 12–14 May 2003) pp 404–5
- [17] Albanese R. and Villone F. 1998 *Nucl. Fusion* **38** 723
- [18] Hofmann F. *et al* 2002 *Nucl. Fusion* **42** 743
- [19] Zohm H. *et al* 2013 *40th EPS Conference on Controlled Fusion and Plasma Physics*
- [20] Biel W. *et al* 2015 *Fusion Eng. Des.* accepted
- [21] Poli E. *et al* 2013 *Nucl. Fusion* **53** 013011
- [22] Poli E., Peeters A. and Pereverzev G. 2001 *Comput. Phys. Commun.* **136** 90–104
- [23] Zohm H. *et al* 2007 *Plasma Phys. Control. Fusion* **49** B341
- [24] Poli E. *et al* 2015 *Nucl. Fusion* **55** 013023
- [25] Figini L. *et al* 2015 *Plasma Phys. Control. Fusion* **57** 054015
- [26] Tsironis C. *et al* 2009 *Phys. Plasmas* **16**
- [27] Kallenbach A. *et al* 2012 *Nucl. Fusion* **52** 122003
- [28] Martin Y.R., Takizuka T. and The ITPA CDBM H-mode Threshold Database Working Group 2008 *J. Phys.: Conf. Ser.* **123** 012033
- [29] Pereverzev G.V. *et al* 1991 *Lab Report* Max-Planck-Institut fuer Plasmaphysik 5/42
- [30] Fable E. *et al* 2013 *Plasma Phys. Control. Fusion* **55** 124028
- [31] Summers H.P. 2004 Atomic data and analysis structure users manual 2.6
- [32] Kallenbach A. *et al* 2013 *Plasma Phys. Control. Fusion* **55** 124041
- [33] Ramogida G. *et al* 2014 *Fusion Eng. Des.* submitted